Detection of Distorted IR-UWB Pulses in Low SNR NLOS Scenarios

Thorsten Wehs, Tilman Leune, Gerd von Cölln, Carsten Koch
Hochschule Emden/Leer, University of Applied Sciences, Germany
Department of Informatics and Electronics
Email: {thorsten.wehs | tilman.leune| gerd.von.coelln | carsten.koch}@hs-emden-leer.de

***Abstract*—In dense environments, for example residential, office or industrial, the predominant type of link within a real time localization system (RTLS) is non-line-of-sight (NLOS). In some NLOS scenarios the signal-to-noise-ratio (SNR) of the first incoming Ultra Wideband (UWB) pulse content is much below 0 dB and the shape of the pulse is distorted. Accordingly the detection of the first pulse is critical. In those cases a possible solution is to detect several sample values which show a high probability to be the center of an UWB pulse. In Time-of-Flight (ToF) based ranging, this leads into a number of pulse or rather distance candidates. The aim of the paper is to present a novel scheme for an improved detection of distorted UWB pulses, especially with SNR below 0 dB. A major objective is to minimize the number of necessary pulse candidates for a defined pulse detection quality. The robustness of the approach has been analyzed by a simulation with a huge number of synthetic pulses in dependency of the SNR and a further series with the degree of distortion as parameter. For a wall of brick and a thickness up to 25 cm an average improvement of 32 % against traditional matched filter (MF) method is achieved.**

I. Introduction

Smart Factory, Industry 4.0, Cyber Physical Systems or Internet of Things require localization systems with fine resolution, good accuracy and especially with a wide area of coverage. In outdoor environments, global navigation satellite systems (GNSS) provide position estimations with accuracies high enough for an increasing number of outdoor applications. Also for indoor environments, the market provides different solutions to localize entities with mobile nodes (or *tags*) attached to them. Localization systems, also called real time locating systems (RTLS), based on the Ultra Wideband (UWB) radio technology show their performance in positioning accuracy since several years [1, 2]. Due to the transmission of very short pulses instead of carrier waves, the ranging accuracy is, compared to other radio technologies, very high. But available RTLS solutions require a fixed set of line-of-sight (LOS) links or links with a weak non-line-of-sight (NLOS) impact between mobile and anchor nodes to provide high accuracies in position estimation. This restriction is a limiting factor for many applications and environments, because the required number of anchor nodes to ensure enough LOS links would have to be unlimited.

In dense environments, for example residential, office or industrial, the predominant type of link is NLOS [3]. Obstacles spatially between anchor and mobile nodes cause bias in range estimation [4, 5] and distortion of the UWB pulse's shape [6]. In addition, the strength of the received signal components is significantly attenuated. In some NLOS scenarios the signal-to-noise-ratio (SNR) of the first incoming pulse content is below 0 dB and accordingly the detection of the first pulse is critical. In those cases a possible solution is to detect several sample values which show a high probability to be the center of the first received pulse as shown in [7]. In Time-of-Flight (ToF) based ranging, this leads to a set of possible pulse candidates, which are further called distance candidates, for each link between anchor and mobile node.

Position estimation, based on traditional least squares need a single determined distance per link. But to detect the first incoming pulse solely without a whole set of candidates, the SNR of the received signal content has to be much higher than 0 dB. The mentioned paradigm results in a complexity trade-off between the traditional least squares methods with single distances and on the other hand the costly maximum likelihood estimation.

A. Motivation

The aim of the paper is to present a novel scheme for the detection of distorted UWB pulses, especially with SNR below 0 dB. A major objective is to minimize the number of required candidates for a defined pulse detection quality. Reducing the set of distance candidates per link leads into a decrease of the computation time due to a smaller number of combinations for least squares method. In addition, by decreasing the amount of combinations, the risk of a false-positive determination, in other words a combination with least residual errors in an incorrect position, is reduced.

B. Related work

There are several approaches for the detection of the first pulse, which differ in terms of complexity and reliability. The simplest method is a threshold-based leading-edge detection (Th-LED) on the raw received signal (waveform) [8]. In Th-LED the first sample above a defined threshold is declared as first received pulse. Predefinition of this threshold is very critical due to the risk of too early (noise) or tardy (multipath component, MPC) detection, reasoned by a too low or a too high threshold. A slight improvement of this method is the usage of a matched filtered (MF) signal instead of the raw waveform (Th-MF-LED). In [9], a further enhancement is shown by applying two centralized average filter to MF signal

with different window widths (adaptive LED). But all these methods may fail in cases of low SNR. But, if distortion of the pulses phase spectrum is weak or moderate, Phase-Only correlators will perform very well [10].

In low SNR scenarios, thresholds for the detection of hidden pulse content have to be much lower than in the proposed methods, which leads to miss-detections or in other words *false-positives*. Therefore, one solution is to detect a number of possible sample values which seem to be the center of an UWB pulse. To address this, an approach proposed in [7], is the gradual increase of the threshold from an early high magnitude sample over the next higher magnitudes to the highest magnitude sample in the waveform finally. This method limits the amount of distance candidates, but excludes scenarios such as a detected noise sample regardless whether in waveform or MF is followed by a pulse with lower magnitude.

A common method which ensures the detection of a low SNR pulse, is to take all peaks in a MF signal above a threshold which is sufficiently low enough. This leads to a large number of distance candidates. As mentioned before, the aim of the paper is to propose an approach to reduce this number without any loss in quality of detection or corresponding, to increase the quality of detection with the same number of distance candidates.

The rest of the paper is structured as follows: In Sec. II the new approach for detection of distorted pulses in a waveform with a method based on amplitude spectrum from frequency domain, is presented. The experimental results and the performance of the proposed algorithm are shown in Sec. III. Sec. IV concludes the paper with an additional outlook.

II. Solution

The proposed approach is based on the hypothesis that the amplitude spectrum of a UWB pulse in many cases is weaker affected by the distortion due to NLOS than the phase spectrum. Therefore, the idea is to take solely the amplitude spectrum of the signal for the pattern matching by correlation. This method is further called |F|-correlation.

The mathematical model for a discrete UWB pulse is:

$$s[t] = A \cdot \left(1 - \frac{4 \cdot \pi \cdot (t - T_c)^2}{\tau^2}\right) \cdot \exp^{-\frac{2 \cdot \pi \cdot (t-T_c)^2}{\tau^2}} \tag{1}$$

where A is the amplitude of the pulse, T_c is the offset on time axis and τ is the characteristic time constant of the UWB pulse [11].

In many localization scenarios, the ideal transmitted pulse $s[t]$ (or $\boldsymbol{s}$) is distorted in its shape and attenuated in its amplitude by a NLOS link. Hence the distorted first pulse $s_{d1}[t]$ (or $\boldsymbol{s_{d1}}$) is, amongst others e. g. multi path components and noise, element of the received waveform $r[t]$.

In [11] the impact of the NLOS case *penetration of a dielectric slab* is described. This NLOS case will be the overall focus of the following considerations. Decisive part of the pulse distortion is the relative shift of the containing frequency components. In this cases the pulses phase spectrum is more affected than the pulses amplitude spectrum. In conjunction to that, the coefficients from |F|-correlation will be higher than the from correlation in time domain where amplitude and phase are combined (further called t-correlation). The correlation coefficient in time domain ρ_t can be described as the Pearson Correlation Coefficient (PCC):

$$\rho_t = \frac{n_t(\boldsymbol{s} \cdot \boldsymbol{s_{d1}}) - (\sum \boldsymbol{s})(\sum \boldsymbol{s_{d1}})}{\sqrt{[n_t(\boldsymbol{s} \cdot \boldsymbol{s}) - (\sum \boldsymbol{s})^2][n_t(\boldsymbol{s_{d1}} \cdot \boldsymbol{s_{d1}}) - (\sum \boldsymbol{s_{d1}})^2]}} \tag{2}$$

where n_t is the length of the pulses, $\boldsymbol{s}$ the transmitted pulse and $\boldsymbol{s_{d1}}$ the received distorted pulse in time domain.

The equivalent PCC correlation in frequency domain ρ_f can be determined as:

$$\boldsymbol{a_s} = a_s[\omega] = |\text{dft}(\boldsymbol{s})| \tag{3}$$

$$\boldsymbol{a_{s_{d1}}} = a_{s_{d1}}[\omega] = |\text{dft}(\boldsymbol{s_{d1}})| \tag{4}$$

$$\rho_f = \frac{n_f(\boldsymbol{a_s} \cdot \boldsymbol{a_{s_{d1}}}) - (\sum \boldsymbol{a_s})(\sum \boldsymbol{a_{s_{d1}}})}{\sqrt{[n_f(\boldsymbol{a_s} \cdot \boldsymbol{a_s}) - (\sum \boldsymbol{a_s})^2][n_f(\boldsymbol{a_{s_{d1}}} \cdot \boldsymbol{a_{s_{d1}}}) - (\sum \boldsymbol{a_{s_{d1}}})^2]}} \tag{5}$$

where n_f is the width of the spectrums $\boldsymbol{a_s}$ and $\boldsymbol{a_{s_{d1}}}$ (typically $n_f = 2^p \geq n_t, p \in \mathbb{N}$), $\boldsymbol{a_s}$ the amplitude spectrum of the transmitted and $\boldsymbol{a_{s_{d1}}}$ the amplitude spectrum of the received pulse. For better readability Eq. 5 is equivalent to:

$$\rho_f = \text{pcc}(\boldsymbol{a_s}, \boldsymbol{a_{s_{d1}}}) \tag{6}$$

According to the hypothesis that correlating amplitude spectrums outperforms correlation in time domain, the condition for an improved detection result is:

$$\rho_f > \rho_t \tag{7}$$

As shown in Fig. 1, the core operation in detection of (possible) first pulses with low SNR in the received waveform $r[t]$ with frequency analysis is a discrete short-time Fourier transform (STFT), which can be described as:

$$X[i,k] = \sum_{m=1}^{n_s} r[m] \cdot w[i-m] \cdot \exp^{-j \cdot \frac{2 \cdot \pi}{N} \cdot k \cdot m} \tag{8}$$

where w is a window function with length l, i is the index of the discrete time position, k is index of the discrete frequencies ($0 \leq k \leq N-1, k \in \mathbb{N}$), m is the running index of waveform $r[t]$, n_s is the length of the received waveform and N is the length of the independent FFTs (typically $N = 2^p \geq l, p \in \mathbb{N}$). For maximum resolution and reducing artifacts at boundaries the step size of windowing in STFT is one sample.

Squaring the magnitudes leads into a spectrogram of the waveform $r[t]$:

$$S[i,k] = |X[i,k]|^2 \tag{9}$$

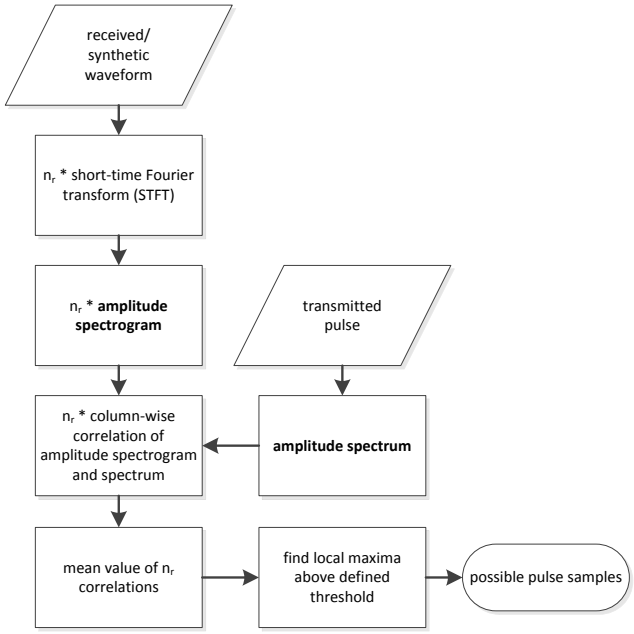

Fig. 1: Flow chart of the proposed scheme for detecting distorted UWB pulses in low SNR scenarios.

For the next step in the algorithm, a column-wise operation on spectrogram S is required, therefore we define $\boldsymbol{C_i}$ as the ith column vector:

$$\boldsymbol{C_i} = \begin{bmatrix} S[i,0] \\ S[i,1] \\ S[i,2] \\ \vdots \\ S[i,N-1] \end{bmatrix} \tag{10}$$

The PCC from spectrogram S and amplitude spectrum of transmitted pulse $\boldsymbol{a_s}$ is defined as follows:

$$\rho_{fS}[i] = \text{pcc}(\boldsymbol{C_i}, \boldsymbol{a_s}) \begin{cases} > 0 & \text{pcc}(\boldsymbol{C_i}, \boldsymbol{a_s}) \\ \leq 0 & 0 \end{cases} \tag{11}$$

To reduce leakage effects in the STFT the steps 8 to 11 are done for n_r different window functions with lengths L ($L = l_1, l_2, \ldots, l_{n_r}$). The correlation vectors $\boldsymbol{\rho_{fS_{n_r}}}$ have to be zero padded, due to the windowing in STFT. These steps lead into a correlation matrix $\rho_{fM}[i,u] (1 \leq u \leq n_r, u \in \mathbb{N})$:

$$\rho_{fM}[i,u] = \begin{bmatrix} \rho_{fS_1}[1] & \rho_{fS_1}[2] & \ldots & \rho_{fS_1}[n_s] \\ \rho_{fS_2}[1] & \rho_{fS_2}[2] & \ldots & \rho_{fS_2}[n_s] \\ \vdots & \vdots & \vdots & \vdots \\ \rho_{fS_{nr}}[1] & \rho_{fS_{nr}}[2] & \ldots & \rho_{fS_{nr}}[n_s] \end{bmatrix} \tag{12}$$

For the final correlation vector $\rho_{fA}[i]$, the matrix $\rho_{fM}[i,u]$ is averaged column-wise ($\boldsymbol{R_i}$):

$$\boldsymbol{R_i} = \begin{bmatrix} \rho_{fM}[1,i] \\ \rho_{fM}[2,i] \\ \vdots \\ \rho_{fM}[n_r,i] \end{bmatrix} \tag{13}$$

$$\rho_{fA}[i] = \overline{\boldsymbol{R_i}} \tag{14}$$

Last step in algorithm, which is illustrated in Fig. 1, is the detection of local maxima $Z[i]$ in correlation result.

$$Z[i] = \text{sgn}[\boldsymbol{\rho_{fA}}']' \begin{cases} < 0 & \text{local maximum} \\ = 0 & \text{other fct. value} \\ > 0 & \text{local minimum} \end{cases} \tag{15}$$

to reduce the number of distance candidates, the maxima can be filtered by a detection threshold:

$$\boldsymbol{P} = \{g : (Z[g] < 0 \text{ and } \rho_{fA}[g] > th_d)\} \tag{16}$$

where th_d is a selectable detection threshold. Finally the vector $\boldsymbol{P}$ is containing the indices of the possible pulse positions in $r[t]$.

III. Experiment and Performance

In this chapter the proposed algorithm is tested by the use of UWB pulses which are distorted by a simulation model. The pulses are embedded in synthetically generated waveforms with an additive white Gaussian noise (AWGN). The improvement and performance is measured by statistical values from a huge number of waveforms in three test perspectives. (1) Quantification of the absolute improvement of |F|-correlation against t-correlation. (2) Behaviour of the detection quality in dependency of a declining SNR. (3) Evidence of the plausibility of the algorithm by the correlation of the general difference between |F|- and t-correlation and the detection quality in dependence of the slab thickness.

In the experiments we are working with pulses which are distorted by a wall of brick. An orthogonal incidence angle on surface of the wall is assumed. The distortion is calculated as mentioned in [6]. Values for the frequency dependent material parameters dielectric constant ϵ_r and loss tangent $\tan\delta$ from 2 GHz to 11 GHz are taken from the paper, too (see Fig. 2). For the pulse template we are using the parameters: $T_c = 0$ and $\tau = 0.134$ ns (cp. Eq. 1). In our consideration the absolute amplitude A of the pulse is irrelevant.

In general, the distortion of the pulse has a strong impact on the shape. Fig. 3 exemplifies the strong influence on the pulse template (blue) by the comparison to a pulse distorted by a 5 cm wall of brick (red). The pulses are represented by 42 samples with a sample interval of 15.625 ps ($f_s = 64$ GHz).

Fig. 4 shows the corresponding amplitude spectrums. The small prongs in the spectrum of the distorted pulse is resulting from the material parameters, where the values were given for sectional frequency slabs of 0.25 GHz (cp. Fig. 2).

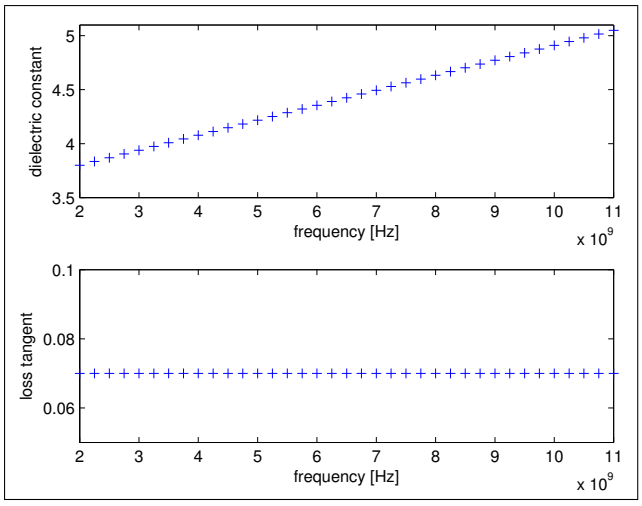

Fig. 2: Frequency dependent material constants dielectric constant ϵ_r and loss tangent $\tan\delta$ for material brick (cp. [6]).

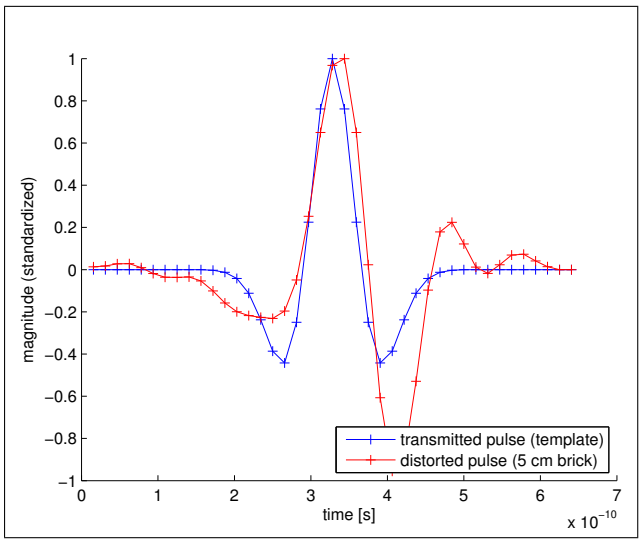

Fig. 3: Simulational results for transmitted pulse template (blue) and pulse distorted by a 5 cm wall of brick (red).

As mentioned in Sec. II, the main idea of our approach is based on the hypothesis that the |F|-correlation outperforms t-correlation for distorted pulses. To confirm this hypothesis, Fig. 5 compares the correlation coefficients in frequency (red) and time domain (blue) over the slab thickness. The slab is made of brick and its thickness varies between 0.5 cm to 25 cm. Fig. 5 indicates, that the coefficient of |F|-correlation is constantly decaying with slab thickness. On the other hand the coefficient of t-correlation has a discontinuous decaying over the slab thickness, which is due to the impact from phase shift and the altering relationship between the frequencies.

The next step in experiment is generation of synthetic waveforms with the distorted pulses. Focus in this paper is to detect stand-alone distorted pulses with no other multi-path or scattering components in the direct neighbourhood. For analysis we selected eleven remarkable slab thicknesses: $[1.5\ 2.5\ 5\ 7\ 8.5\ 10\ 12\ 13\ 17\ 20\ 22.5]$ cm from Fig. 5. For

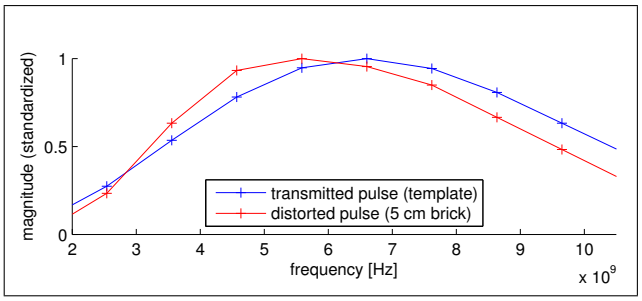

Fig. 4: Simulational results for amplitude spectrum of transmitted pulse template (blue) and pulse distorted by a 5 cm thick wall of brick (red).

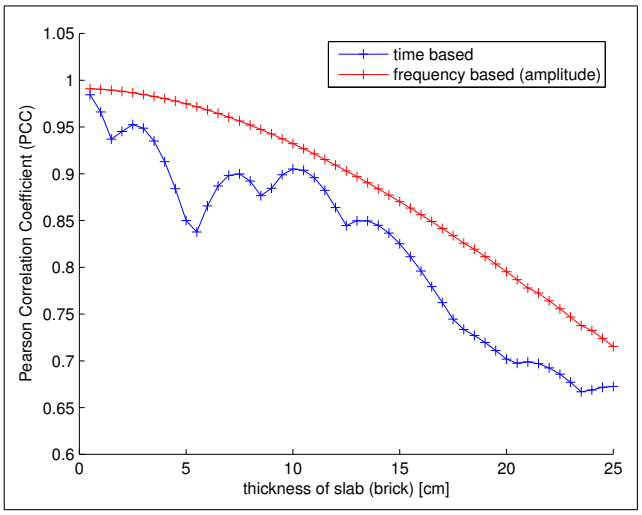

Fig. 5: Comparison of the correlation coefficients (PCC) t-correlation vs. |F|-correlation over the thickness of slab. For instance at 5 cm: PCC of signals in Fig. 3 vs. PCC of spectrums in Fig. 4.

each thickness, 100 exemplary waveforms were generated and each waveform contained three pulses with a random amplitude factor and an AWGN $N(0,\sigma^2)$ with constant σ. This leads to eleven sets with each 300 noisy pulses with SNR between approximately -35 dB and -5 dB in our case. The overall length of the waveforms is 100 ns with a gap of 25 ns between the distorted pulses.

Fig. 6 shows a small part of about 2 ns of the correlation results on a synthetic waveform scan. The black and magenta lines show the distorted pulses with and without AWGN. The true position of the pulse is marked by a cyan vertical line ($t = -25.02$ ns Fig. 6). The red line marks the correlation coefficients $\rho_{fA}[i]$ resulting from Eq. 14. In this example the number of window functions is $n_r = 3$ with lengths $L = \{40, 60, 70\}$ (cp. Eq. 12). After determination of local maxima (cp. Eq. 16) the maxima respectively distance candidates are filtered by a defined detection threshold. The threshold (green dashed line) is calculated dynamically for each waveform and has the maximum value in which the three distorted pulses are detected in the specific waveform. This leads into an array P_f (cp. Eq. 16) of distance candidates (red marker) which includes

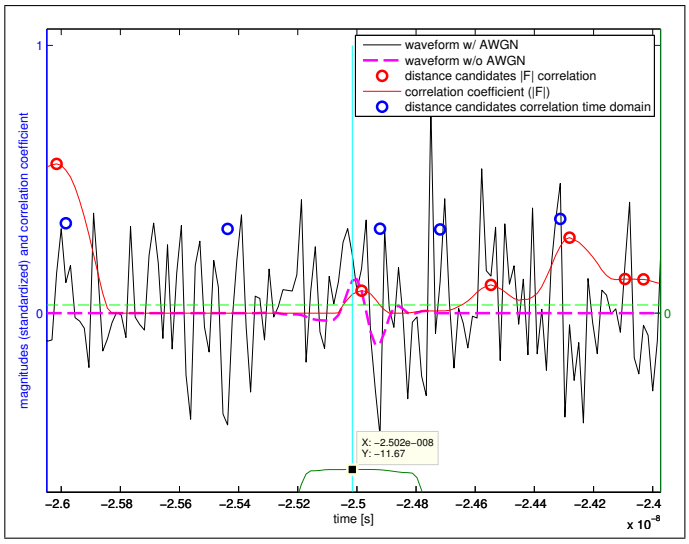

Fig. 6: Example of a correlation result with coefficients from |F|-correlation (red line), distance candidates from |F|-correlation (red markers) and distance candidates from t-correlation (blue markers). It is shown a small part of a waveform with 5 cm slab thickness and one pulse with a SNR of -11.67 dB. Vertical cyan line at $t = -25.02$ ns marks the true position of the pulse and the horizontal green dashed line marks the detection threshold for distance candidates in frequency domain.

some false-positives typically in case of low SNR and the three detections of the distorted pulses for each waveform.

To benchmark the proposed algorithm, the distance candidates will be compared to candidates resulting from t-correlation. Basis for the benchmark is to evaluate which algorithm performs more accurate with a given amount of distance candidates. The number of candidates for |F|-correlation is already defined by the length of P_f and varies for each waveform. To get an opposing array of distance candidates for t-correlation P_t, the same amount of candidates in form of the highest correlation coefficients in time domain for each waveform is taken (see blue marker in Fig. 6). To summarize this, for each waveform there are two arrays with distance candidates P_f and P_t which have the same length.

The criterion to quantify the quality of distance candidates is the deviation of the nearest candidate to the true positions of distorted pulses. For example, in Fig. 6 the deviation for the nearest red candidate is 2 samples and the deviation of the blue candidate is 6 samples. This deviation is calculated with P_f and P_t for all 300 distorted pulses per slab thickness. The statistical result for the slab thickness 5 cm is presented in Fig. 7. The 300 pulses are divided in 15 different SNR classes of 2 dB width. For each SNR class the mean and median value of the deviation of the nearest candidates is calculated.

In this case the median and mean values of the |F|-correlation are visibly below the t-correlation. To quantify the improvement the SNR class values were integrated: $|\mathrm{F}|_{median,5cm} = 142.5$ samp., $\mathrm{t}_{median,5cm} = 217.0$ samp.,

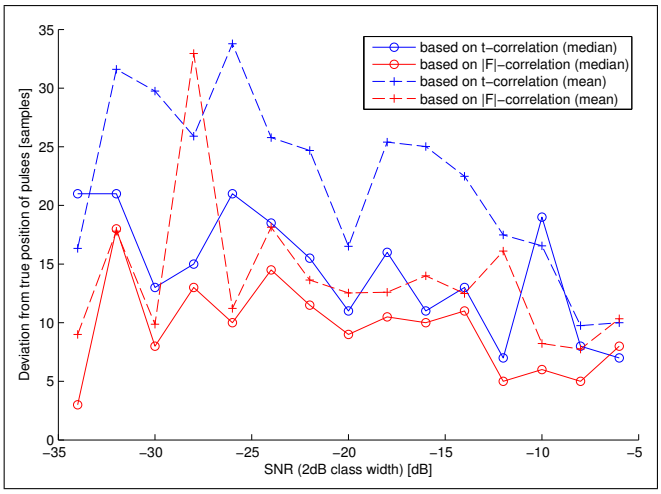

Fig. 7: Benchmark of detection quality between t-correlation and |F|-correlation for a slab thickness of 5 cm. Quality criterion is the deviation of detections to the true pulse positions. The mean and median values for the deviation are printed over the SNR of the pulses.

$|\mathrm{F}|_{mean,5cm} = 206.7$ samp., $\mathrm{t}_{mean,5cm} = 330.7$ samp. This lead into ratios for improvement:

$$\mathrm{Rat}_{\mathrm{median,5\ cm}} = \frac{|\mathrm{F}|_{\mathrm{median,5\ cm}}}{\mathrm{t}_{\mathrm{median,5\ cm}}} = \frac{142.5\,\mathrm{samp.s}}{217.0\,\mathrm{samp.s}} = 0.65 \quad (17)$$

$$\mathrm{Rat}_{\mathrm{mean,5\ cm}} = \frac{|\mathrm{F}|_{\mathrm{mean,5\ cm}}}{\mathrm{t}_{\mathrm{mean,5\ cm}}} = \frac{206.7\,\mathrm{samp.s}}{330.7\,\mathrm{samp.s}} = 0.63 \quad (18)$$

This values show an improvement in detection accuracy of about 35 % ($1 - \mathrm{Rat}_{\mathrm{median,5\ cm}}$). This means, with the same amount of distance candidates the deviation decreases to 65 % of the t-correlation. In many cases the $\mathrm{Rat}_{\mathrm{mean}}$ is much smaller than the $\mathrm{Rat}_{\mathrm{median}}$, because sometimes in P_t no distance candidate is in the near neighbourhood of the true position. So actually in those cases the pulse is not detected by the algorithm and the nearest pulse is a false-positive detection in noise around the true position, e. g. if the blue marker third from left in Fig. 6 is missing. This leads into an outlier and a higher mean value in the corresponding SNR class and thus in $\mathrm{t}_{\mathrm{mean,thickness}}$, too.

In Fig. 8 the relation between the basis ratio of correlation (blue line) and $\mathrm{Rat}_{\mathrm{mean,thickness}}$ of the deviations over the slab thickness is shown. The basis ratio could be calculated from Fig. 5 as follows:

$$\mathrm{Rat}_{\mathrm{basis,thickness}} = \frac{\mathrm{pcc}_{\mathrm{t,thickness}}}{\mathrm{pcc}_{|\mathrm{F}|,\mathrm{thickness}}} \quad (19)$$

For instance the basis correlation ratio for 5 cm slab thickness $\mathrm{Rat}_{\mathrm{basis,5\,cm}}$ is:

$$\mathrm{Rat}_{\mathrm{basis,5\,cm}} = \frac{\mathrm{pcc}_{\mathrm{t,5\,cm}}}{\mathrm{pcc}_{|\mathrm{F}|,\mathrm{5\,cm}}} = \frac{0.845}{0.974} = 0.867 \quad (20)$$

The values for different $\mathrm{Rat}_{\mathrm{mean}}$ are calculated in an extensive simulation run for two configurations: one window in

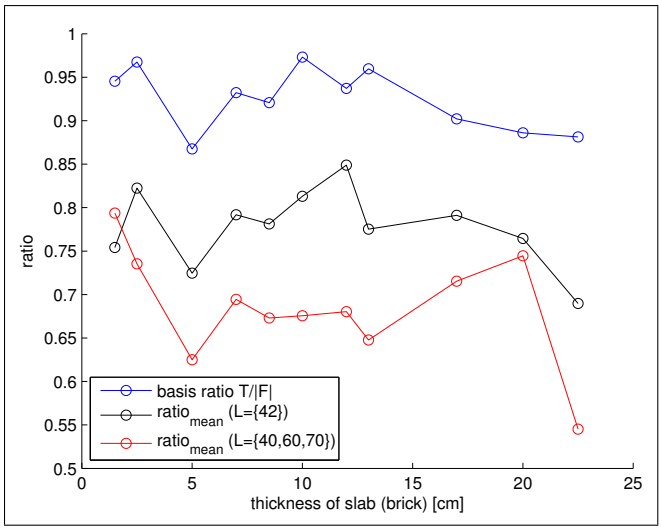

Fig. 8: Comparison of the basis correlation ratio $\mathrm{Rat}_{\mathrm{basis,thickness}}$ (cp. Fig. 5 and Eq. 20) and $\mathrm{Rat}_{\mathrm{mean,thickness}}$ with one window ($L = \{42\}$) and three windows ($L = \{40, 60, 70\}$) over the slab thickness for eleven remarkable thicknesses.

STFT ($L = \{42\}$, black line) and three windows in STFT ($L = \{40, 60, 70\}$, red line). As expected, the accuracy of pulse detection is almost exactly following the basis correlation ratio over the thickness of the slab. The mean value of the $\mathrm{Rat}_{\mathrm{mean}}$ over range of slab thickness is about $68\,\%$ (three window sizes). The impact through more and wider windows in STFT leads in an improvement of additional 12 percent points towards the one-window run.

IV. Conclusion

In indoor environments UWB pulses are often strongly distorted and attenuated by the penetration through walls or other obstacles. This leads into very low SNR of the pulses in received waveforms. This paper presented a novel approach for the improved detection of distorted low SNR UWB pulses. The aim was to reduce the amount of distance candidates needed for a defined detection quality, which would reduce the computation time and the risk of false-positives in position estimation. The algorithm is logically based on higher correlation coefficients of amplitude spectrums in frequency domain towards the MF correlation in time domain. Technically the core of the algorithm is a short-time Fourier transform with different window sizes.

It was shown that there is a varying gap between the correlation coefficients of |F|-correlation and t-correlation depending on the thickness of the penetrated wall. Furthermore the averaged improvement of the detection accuracy for a wall of brick was quantified for eleven different thicknesses with a SNR range of $-35\,\mathrm{dB}$ to $-5\,\mathrm{dB}$. In mean the detection quality was improved by $32\,\%$ $\left(1 - \overline{\mathrm{Rat}}_{\mathrm{mean,thickness,L=\{40,60,70\}}}\right)$ for the simulation run with three window sizes in STFT.

Next steps in the work are the development of further evaluation criteria and the adoption of other materials and pulse shapes. Another aspect is the investigation of the impact of varying the incidence angle on the slab. A test of the algorithm on real world waveform scans is likewise pending for the future.

Acknowledgment

The authors would like to thank the European Regional Development Fund (ERDF) to give us the possibility to research at such an interesting and innovative subject.

References

[1] T. Phebey, "The Ubisense Assembly Control The Ubisense Assembly Control Solution for BMW," in *RTLS in Manufacturing Workshop - RFID Journal Europe Live!*, 2010.

[2] Zebra Technologies, Ed., *Zebra Dart Ultra-Wideband Brochure*, 2010.

[3] Maranò, S., W. Gifford, H. Wymeersch, and M. Win, "NLOS identification and mitigation for localization based on UWB experimental data," *IEEE Journal on Selected Areas in Communications*, vol. 28, no. 7, 2010.

[4] D. Dardari, A. Conti, U. Ferner, A. Giorgetti, and M. Win, "Ranging With Ultrawide Bandwidth Signals in Multipath Environments," *Proceedings of the IEEE*, vol. 97, no. 2, pp. 404–426, 2009.

[5] C. Chen, D. Hong, H. Xiaotao, L. Xiangyang, and Y. Jibing, "Through-wall localization with UWB sensor network," in *Ultra-Wideband (ICUWB), 2012 IEEE International Conference on*, 2012, pp. 284–287.

[6] M. Jing, Y. Z. Qin, and T. Z. Nai, "Impact of IR-UWB waveform distortion on NLOS localization system," in *Ultra-Wideband, 2009. ICUWB 2009. IEEE International Conference on*, 2009, pp. 123–128.

[7] S. Guowei, R. Zetik, Y. Honghui, O. Hirsch, and R. Thoma, "Time of arrival estimation for range-based localization in UWB sensor networks," in *Ultra-Wideband (ICUWB), 2010 IEEE International Conference on*, vol. 2, 2010, pp. 1–4.

[8] K. Haneda, K. i. Takizawa, J. i. Takada, M. Dashti, and P. Vainikainen, "Performance evaluation of threshold-based UWB ranging methods - Leading edge vs. search back -," in *Antennas and Propagation, 2009. EuCAP 2009. 3rd European Conference on*, 2009, pp. 3673–3677.

[9] M. Kuhn, J. Turnmire, M. Mahfouz, and A. Fathy, "Adaptive leading-edge detection in UWB indoor localization," in *Radio and Wireless Symposium (RWS), 2010 IEEE*, 2010, pp. 268–271.

[10] Z. Yuan, L. G. Yong, C. Law, and X. Chi, "High-Resolution UWB Ranging based on Phase-Only Correlator," in *Ultra-Wideband, 2007. ICUWB 2007. IEEE International Conference on*, 2007, pp. 100–104.

[11] M. Jing, Z. Nai-tong, and Z. Qin-yu, "IR-UWB Waveform Distortion Analysis in NLOS Localization System," *Information Technology Journal*, vol. 9, no. 1, pp. 139–145, 2010.